MOLECULAR AND CELLULAR BIOLOGY, July 1991, p. 3545–3553
0270-7306/91/073545-09$02.00/0

Vol. 11, No. 7

In Vivo Characterization of the *Saccharomyces cerevisiae* Centromere DNA Element I, a Binding Site for the Helix-Loop-Helix Protein CPF1

RAINER NIEDENTHAL, REGINE STOLL, AND JOHANNES H. HEGEMANN*

Institut für Mikrobiologie und Molekularbiologie, Justus-Liebig-Universität, Frankfurter Strasse 107, 6300 Giessen, Federal Republic of Germany

Received 7 January 1991/Accepted 11 April 1991

The centromere DNA element I (CDEI) is an important component of *Saccharomyces cerevisiae* centromere DNA and carries the palindromic sequence CACRTG (R = purine) as a characteristic feature. In vivo, CDEI is bound by the helix-loop-helix protein CPF1. This article describes the in vivo analysis of all single-base-pair substitutions in CDEI in the centromere of an artificial chromosome and demonstrates the importance of the palindromic sequence for faithful chromosome segregation, supporting the notion that CPF1 binds as a dimer to this binding site. Mutational analysis of two conserved base pairs on the left and two nonconserved base pairs on the right of the CDEI palindrome revealed that these are also relevant for mitotic *CEN* function. Symmetrical mutations in either half-site of the palindrome affect centromere activity to a different extent, indicating nonidentical sequence requirements for binding by the CPF1 homodimer. Analysis of double point mutations in CDEI and in CDEIII, an additional centromere element, indicate synergistic effects between the DNA-protein complexes at these sites.

For faithful transmission of genetic material in eucaryotes, two main processes are responsible: mitosis and meiosis. During these processes, the duplicated chromosomes become attached to the spindle fibers and subsequently segregate in an orderly fashion to mother and daughter cells. Attachment of the chromosomes to the spindle occurs via the kinetochore at a specific chromosomal segment termed the centromere. The centromere DNA (*CEN* DNA) is bound by specific centromere proteins and is thought to be the organizing center for the kinetochore. So far, only for the yeasts *Saccharomyces cerevisiae* and *Schizosaccharomyces pombe* has it been possible to isolate centromere DNA (13–15, 39, 40). In the budding yeast *S. cerevisiae*, all meiotic and mitotic centromere functions required in *cis* are contained within a 125-bp *CEN* DNA fragment (16). This fragment comprises three centromere DNA elements (CDEI, CDEII, and CDEIII) conserved throughout the 13 *CEN* DNAs that have been isolated thus far (19, 27, 29, 30a) (Fig. 1). Chromatin analysis has uncovered a specific centromere chromatin structure (5). A detailed analysis revealed a region of approximately 160 bp, including CDEI, CDEII, and CDEIII, which is protected against nuclease digestion (20). In vivo footprint analysis identified specific G nucleotides within CDEI and CDEIII as protected against methylation, indicating tight DNA-protein interactions at these sites (36, 50).

The first evidence that the CDEI sequence RTCACRTG (R = purine) may act as a protein-binding site was presented by Bram and Kornberg, who identified an activity in partly purified yeast protein extracts which bound not only to the CDEI sequence in the centromere, but also to a CDEI sequence found in the *GAL2* promoter (6). Subsequently, other groups purified this protein, referred to variously as CPF1 (centromere and promoter factor), CP1 (centromere protein), and CBF1 (centromere-binding factor), and cloned its gene (2, 3, 8, 9, 31, 36). Recently, direct evidence was provided that the same protein can bind to these CDEI sites in centromeres and promoters, although their role in transcriptional regulation is still unclear. Deleting the gene leads to changes in chromatin structure and in vivo footprint pattern (36) as well as to functional changes at promoter and centromere sites (methionine auxotrophy and increased mitotic chromosome loss rate [3, 9, 36]). This CDEI-binding protein belongs to a group of sequence-specific DNA-binding proteins characterized by a helix-loop-helix (HLH) domain, which is thought to be involved in protein dimerization (38). It was shown that this protein, referred to here as CPF1, binds in vitro to CDEI as a homodimer (36). In higher eucaryotes, members of the HLH protein family are involved in transcriptional regulation and in the control of cell differentiation and cell proliferation, binding to DNA either as homodimers or heterodimers with other members of this family (7, 38). They all recognize DNA sequences containing in their central part the palindrome CACGTG or variants of this sequence which fit the general consensus sequence CANNTG (e.g., USF [46]; TFEB [10]; TFE3 [4]; MyoD [38]; and myf5 [7]).

Deletion of the centromere DNA element I containing the hexanucleotide CACRTG revealed that this site plays an important role in mitotic and meiotic centromere function (17, 22, 45). Moreover, the change of two different base pairs in the right half-site of the CDEI palindrome affects mitotic centromere function (25). In higher eucaryotic promoters, two different point mutations in the palindromic binding site CACGTG of the *Xenopus* TFIIIA distal element factor resulted in a reduction in TFIIIA promoter activity in oocytes (23), and a double mutation in the left half-site of the same sequence inhibited binding of the human TFEB protein in vitro (10).

In order to characterize this widespread protein-binding motif, we performed saturation mutagenesis of CDEI with the aim of quantifying the contribution of all base pairs in the palindrome to mitotic *CEN* function. With respect to the

* Corresponding author.

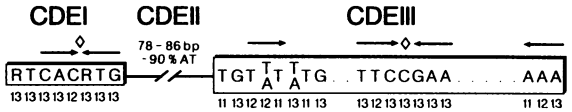

FIG. 1. Centromere consensus sequence. The DNA sequences of 13 centromeres (*CEN1* through *CEN7*, *CEN10*, *CEN11*, and *CEN13* through *CEN16*) from *S. cerevisiae* were compared, resulting in the consensus sequence RTCACRTG (27, 29, 30a) (*CEN2*), which consists of the three centromere DNA elements CDEI, CDEII, and CDEIII (R = purine). Numbers indicate the degree of conservation (e.g., 13 indicates that the nucleotide appears in 13 centromeres at this position). Positions with a nonconserved nucleotide are represented by dots. Palindromic structures are indicated by arrows together with a diamond, which represents the twofold symmetry axis.

consensus sequence CANNTG, the central base pairs in CDEI were of special interest. In addition, we mutated the adjacent 2 bp left and right of the CDEI palindrome. We expected to obtain further hints to the type of interaction that occurs between CDEI and the CPF1 protein dimer.

The in vivo analysis of CDEI mutations was performed with a rapid colony-sectoring assay and a highly sensitive cycloheximide resistance/sensitivity (R/S) system, which rely on a colony color assay for chromosome stability (26) and a method for creating artificial chromosome fragments, as described earlier (25, 48). The results confirm the importance of all palindromic CDEI base pairs for mitotic *CEN* function but in addition show that the base pairs at positions 9 and 10 (Fig. 2A) are relevant for complete centromere activity. The left palindromic half-site is more relevant for faithful chromosome segregation than the right half-site. One perfect 10-bp-long CDEI palindrome carrying three changes compared with the wild-type sequence has a *CEN* activity nearly as effective as that of wild-type *CEN6*-CDEI, indicating second-site suppression in this protein-binding site. Finally, mutants with mutations in both CDEI and CDEIII point to interactions between the CDEI and CDEIII DNA-protein complexes.

(This research was conducted by R.N. in partial fulfillment of the Ph.D. degree requirements.)

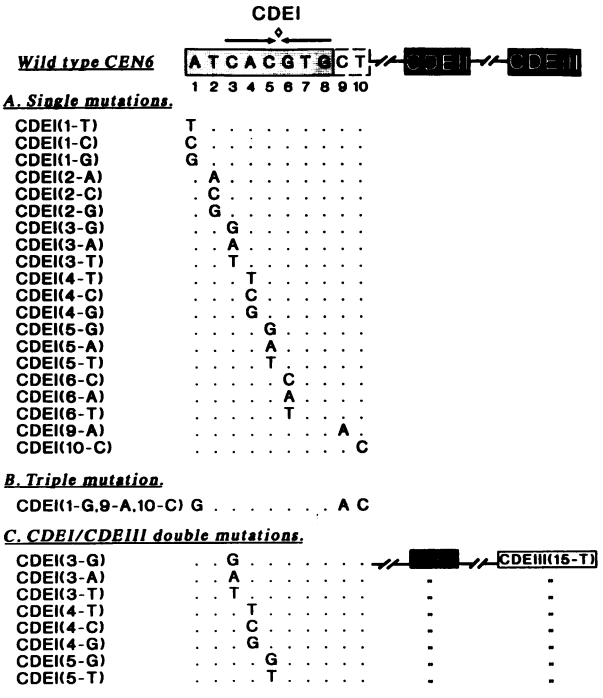

FIG. 2. List of mutations created in this study. The conserved CDEI sequence is marked by a shaded box, with the palindrome and the symmetry axis indicated, while the dotted-line box marks the enlargement of CDEI, as discussed in the text. Numbers below each nucleotide mark the position to facilitate mutant identification (25). Unaltered nucleotides are indicated by dots.

MATERIALS AND METHODS

Media, chemicals, and enzymes. The different nonselective (YPD) and selective (SD) media for the yeast strains and the media (YT and M9) for bacteria were as described previously (25). Medium components were from Difco Laboratories, GIBCO Laboratories, and Sigma Chemical Co. Restriction enzymes, T4 DNA ligase, polynucleotide kinase, and DNA polymerase were purchased from various companies and were used under the conditions suggested by the suppliers.

Cells. *Escherichia coli* BMH71-18*mutS* [*supE thi mutS 215*::Tn*10* Δ(*lac-proAB*) F′ (*proAB*$^+$ *lacI*^{q} *lacZ*ΔM15)] and MK30-3 [*recA galE strA* Δ(*lac-proAB*) F′ (*proAB*$^+$ *lacI*^{q} *lacZ*ΔM15)] were obtained from H. J. Fritz. *E. coli* JM101 [*supE thi* r_K^+ m_K^+ Δ(*lac-proAB*) F′ (*proAB*$^+$ *lacI*^{q} *lacZ*ΔM15 *traD36*)] was obtained from J. Messing. *E. coli* XL1-Blue {*supE44 hsdR17 recA1 endA1 gyrA46 thi relA1 lac* F′ [*proAB*$^+$ *lacI*^{q} *lacZ*ΔM15::Tn*10* (Tet^r)]} was purchased from Stratagene.

S. cerevisiae YPH49 [**a**/α *ura3-52*/*ura3-52 lys2-801*(Am)/*lys2-801*(Am) *ade2-101*(Oc)/*ade2-101*(Oc) *trp1*-Δ*1*/*trp1*-Δ*1*] was obtained from P. Hieter. YJH6 is identical to YPH49 but is cycloheximide resistant (*cyh*^{r}*2*/*cyh*^{r}*2*) and was obtained from A. Wilmen.

Plasmids and oligonucleotides. M13mp9 and M13mp9 rev were obtained from H. J. Fritz. pKE5 was constructed by cloning a 1.4-kb *Bam*HI-*Hin*dIII *CYH*^{s}*2* DNA (source: J. R. Warner) in the *Bam*HI-*Hin*dIII sites of pYCF5 (25).

The oligonucleotides were synthesized with the Applied Biosystem DNA synthesizer 380B with phosphoramidite chemistry. All oligonucleotides used for oligonucleotide-directed mutagenesis are listed in Table 1. For sequence analysis of the mutants, an oligonucleotide called oligo XIX, d(TAATGCTAAATACTC), binding 78 bp upstream of CDEI, was used.

Oligonucleotide-directed mutagenesis. The creation of CDEI and CDEI-CDEIII mutations was performed by the gapped-duplex DNA approach (33) exactly as described by Hegemann et al. (25). To obtain the CDEI-CDEIII double mutations, a gapped-duplex DNA of the already available CDEIII(15-T) mutation (25) was prepared. Mutagenesis was performed with an equimolar mixture of the CDEI oligonucleotides XVI, XVII, XXVI, XXVII, XXX, and XXXI. Identification of *CEN6* single mutations was done by a dot-blot hybridization with the mutagenic ^{32}P-labeled oligonucleotide. For identification of dcuble mutations in CDEI and CDEIII, a dot-blot hybridization with a CDEI wild-type (wt) oligonucleotide was performed. All potential mutants were finally defined by dideoxy sequence analysis with the T7 polymerase (Pharmacia) or Sequenase version 2 (USB) kit.

Determination of mitotic chromosome fragment loss rates. We measured the centromere activity of the *CEN* mutants

TABLE 1. Oligonucleotides used for creation of mutations

Oligonucleotide	Sequence[a] (5'→3')	Position changed in CDEI[b]
XVI	TCATCACG(A,C,G)GCTATAAA	7-T
XVII	CATCACGT(A,C,T)CTATAAAA	8-G
XXVI	TTTCATCA(A,G,T)GTGCTATA	5-C
XXVII	TTCATCAC(A,C,T)TGCTATAA	6-G
XXVIII	TTCTTTTC(C,G,T)TCACGTGC	1-A
XXIX	TCTTTTCA(A,C,G)CACGTGCT	2-T
XXX	CTTTTCAT(A,G,T)ACGTGCTA	3-C
XXXI	TTTTCATC(C,G,T)CGTGCTAT	4-A
LXI	TCACGTGCCATAAAAAT	10-T
LXII	ATCACGTGATATAAAAA	9-A
LXV	TCTTTTCACCACGTGCT	2-T
LXIX	CGTCACGTGACATAAAAATA	1-A/9-C/10-T
LXX	TTTTCATCCCGTGCTAT	4-A
LXXI	TTCTTTTC(C,T)TCACGTGC	1-A

[a] Underlined nucleotides are different from the wt CDEI sequence. Nucleotides in parentheses represent mixed positions.

[b] The CDEI sequence is numbered to facilitate identification of a particular base pair (25) (see Fig. 2, top).

TABLE 2. Colony-sectoring phenotype assay[a]

Mutation	Colony phenotypes (avg, %), red/h.sec/l.sec/pink	Mitotic chromosome fragment loss rate[b]
Reference list		
wt *CEN6*	0/0/10/90	4.8×10^{-4}
CDEI(7-C)	0/0/14/86	8.1×10^{-4}
CDEI(7-G)	0/0/50/50	1.3×10^{-3}
CDEI(8-A)	0/8/54/38	2.1×10^{-3}
CDEI(8-C)	0/9/73/18	4.0×10^{-3}
CDEIII(19V20-G)	0/100/0/0	9.6×10^{-3}
CDEIII(15-T)	11/89/0/0	1.1×10^{-1}
New CDEI mutants		
CDEI(6-A)	0/0/20/80	8.1×10^{-4}–1.3×10^{-3}
CDEI(6-C)	0/0/29/71	8.1×10^{-4}–1.3×10^{-3}
CDEI(5-T)	0/0/33/67	8.1×10^{-4}–1.3×10^{-3}
CDEI(5-G)	0/0/50/50	1.3×10^{-3}–2.1×10^{-3}
CDEI(4-T)	0/0/60/40	1.3×10^{-3}–2.1×10^{-3}
CDEI(4-G)	0/0/67/33	1.3×10^{-3}–2.1×10^{-3}
CDEI(6-T)	0/17/67/16	4.0×10^{-3}–9.6×10^{-3}
CDEI(5-A)	33/50/17/0	9.6×10^{-3}–2.2×10^{-1}

[a] Yeast transformants carrying the chromosome fragment with wt or mutated *CEN6* were plated onto six nonselective SD plates to yield about 50 colonies per plate and incubated for 5 days at 30°C. With a magnifier, we scored the number of red, highly sectored (more than 25 red sectors [h.sec]), low sectored (less than 25 red sectors [l.sec]), and pink colonies and calculated the ratios.

[b] The mitotic chromosome fragment loss rates for the constructs in the reference list were taken from Hegemann et al. (25) and recalculated as mentioned in Materials and Methods. The mitotic chromosome fragment loss rates of the new mutants were deduced from the reference list by comparing their colony-sectoring phenotype with those of the constructs from the reference list.

on an artificial chromosome (25). All mutations were cloned as 1.16-kb *Bam*HI-*Sal*I fragment into the chromosome fragmentation vector pKE5. Additionally, the mutations CDEI (4-G), CDEI(4-T), CDEI(5-A), CDEI(5-G), CDEI(5-T), CDEI(6-A), CDEI(6-C), and CDEI(6-T) were cloned into the fragmentation vector pYCF5 (25). For transformation and chromosome fragmentation, the *CEN6* mutants carrying the vectors were linearized with *Not*I and transformed by the lithium acetate method (30) into yeast cells. After selection for uracil prototroph transformants on minimal SD plates, four transformants of each mutation were checked by orthogonal field alteration gel electrophoresis (OFAGE) analysis for the presence of a chromosome fragment (CF) of about 125 kb. For each mutation, one transformant with the karyotype $2n$ + CF was tested for mitotic chromosome fragment stability.

Test systems for determining mitotic chromosome fragment loss rate. (i) System I: quantitative comparison of colony sectoring. The yeast strains YPH49 and YJH6 are homozygous for the mutation *ade2-101*, while the chromosome fragment carries the *SUP11* gene (26). We set up a reference list of mutants with known chromosome fragment loss rates (Table 2). By comparing the phenotypes of new *CEN* mutants with those of the mutants on this list, we determined the chromosome fragment loss rate of the mutants (Table 2).

(ii) System II: cycloheximide R/S system. To establish the R/S system, we isolated a cycloheximide-resistant mutant of YPH49 called YJH6 (51). Transformation of YJH6 with linearized pKE5, which carries the dominant cycloheximide sensitivity allele and the *CEN6* variants, leads to cycloheximide-sensitive, uracil-prototrophic transformants. After identification of a chromosome fragment-carrying transformant by OFAGE, selectively grown cells were plated on nonselective SD plates. Following 36 h of incubation at 30°C, 10 colonies with the same generation number (colony size measured under the microscope) were picked and resuspended in 500 μl of distilled water. Of this suspension, 2% was plated on five YPD plates, and the remaining 98% was plated on two YPD-cycloheximide (10 μg/ml) plates. The YPD plates were incubated at 30°C for 3 days, and the YPD-cycloheximide plates for 5 days. By counting the colonies on the YPD plates, we could evaluate the colony size. By counting the colonies on the YPD-cycloheximide plates, we determined the number of cells which had lost the chromosome fragment. The rate of loss per mitotic cell division was obtained by the method of the median (fluctuation analysis [35]) as described by Hegemann et al. (25). The chromosome fragment loss rate for wt *CEN6* in the yeast strain YJH6 was about 2.53-fold higher than the loss rate in strain YPH49 (25) (data not shown). For comparison, the mitotic chromosome fragment loss rates of CDEI mutants analyzed in YPH49 were multiplied by 2.53 (Table 2; see Fig. 4).

(iii) System III: estimation of percentage of chromosome fragment-carrying cells in selective medium. The loss rate of the double CDEI-CDEIII mutants was too high to allow quantification with the cycloheximide R/S system. We therefore estimated, for eight double mutants, the corresponding single CDEI mutants, and for the single CDEIII(15-T) mutant, the percentage of cells which, under selective conditions, carried a chromosome fragment. We set up 10 cultures for each mutant, allowed growth for 4 to 5 days in selective liquid medium to the stationary phase, and plated equal numbers of cells (100 to 200) on two nonselective and two selective SD plates. By counting the colonies growing on these plates, we determined the percentage of cells which carried a chromosome fragment under selective conditions and calculated the mean value together with the standard deviation.

RESULTS

Design of CDEI mutations. The centromere sequence in the budding yeast *S. cerevisiae* consists of the three conserved DNA elements CDEI, CDEII, and CDEIII, dia-

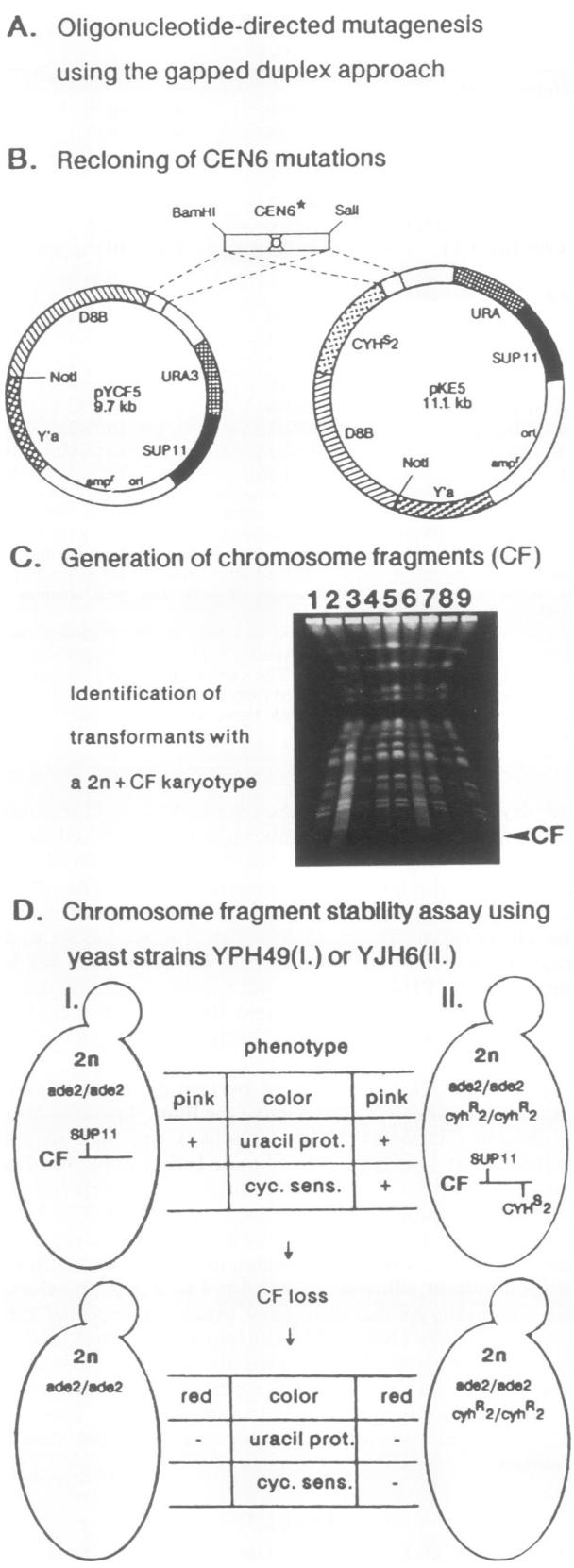

FIG. 3. Schematic representation of the steps involved in the analysis of mutated *CEN6* DNAs. (A) All point mutations created in this study were prepared by oligonucleotide-directed mutagenesis by the gapped-duplex approach (33). (B) The mutated *CEN6* DNAs were recloned into the fragmentation vectors pYCF5 and pKE5. After linerization at the unique *Not*I site, the plasmids were transformed into yeast cells. Upon interactions between the linear plasmid ends and the homologous yeast sites, a new artificial chromosome fragment (CF), about 125 kb in size, is generated. (C) This molecule can be visualized by OFAGE analysis as a new chromosomal band (arrow CF). The karyotype of the parental strain YJH6 is shown in lane 1, while lanes 2 through 9 represent individual transformants all exhibiting the chromosome fragment. (D) I. Transformation of diploid yeast strain YPH49 with plasmids derived from pYCF5 allows monitoring of chromosome fragment segregation by analysis of individual colonies for two phenotypes, pink color and uracil prototrophy. Loss of the chromosome fragment results in red, uracil-auxotrophic colonies. II. Likewise, transformation of pKE5-derived plasmids into the diploid yeast strain YJH6 results in pink, uracil-prototrophic (prot.), and cycloheximide-sensitive (cyc. sens.) colonies. Chromosome fragment loss leads to colonies which are red, uracil auxotrophic, and cycloheximide resistant. (Further details to each step are discussed in Materials and Methods.)

grammed in Fig. 1. The CDEI DNA sequence is highly conserved, showing a palindromic structure covering 6 bp (positions 3 to 8) and two additional conserved base pairs at the left side of the dyad (positions 1 and 2). In order to rigorously quantify the contribution of each palindromic base pair within CDEI as well as of the adjacent 2 bp left and right to mitotic centromere function, we introduced 20 single point mutations at positions 1 to 10 of CDEI from *CEN6*, as listed in Fig. 2A, and analyzed their ability to function in mitotic chromosome segregation. To understand more about the influence of the dyad structure for CPF1 binding, we designed two different 10-bp-long perfect palindromic CDEI versions by changing either one or three positions, respectively (Fig. 2A and B).

Although the two DNA-protein complexes located at CDEI and CDEIII are separated by CDEII, early data suggested an interaction between both complexes (45). Therefore, we created a series of CDEI-CDEIII double mutants. To the primary mutation CDEIII(15-T), which was shown to severely reduce centromere activity (25), we added eight different CDEI point mutations at positions 3 to 5, all belonging to the left half of the CDEI palindrome and affecting *CEN* function to various degrees (Fig. 2C). The various mutations were introduced via site-directed mutagenesis with the oligonucleotides listed in Table 1 and following the gapped-duplex approach (33) (Fig. 3).

In vivo test systems for analyzing *CEN* mutants. The test systems used to quantify the ability of a centromere DNA to participate in mitotic chromosome segregation employ genetically marked artificial chromosome fragments as described previously (25, 48). For this, we cloned the CDEI mutants as 1.16-kb *Bam*HI-*Sal*I fragments into plasmids pYCF5 and pKE5 (Fig. 3B). After linearization and transformation into yeast cells, the vector ends undergo homologous recombination via the Y'a and the chromosome 3-specific D8B sequence. As a result, a 125-kb chromosome fragment is generated, derived from the left arm of chromosome 3. The presence of the new nonessential chromosome fragment was verified by OFAGE analysis (Fig. 3C). The segregation of the chromosome fragment can be monitored by following the chromosome fragment-encoded *SUP11* marker.

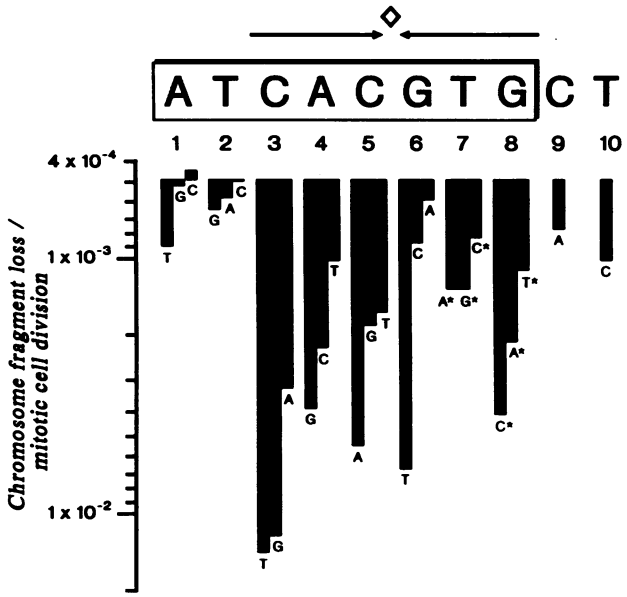

FIG. 4. Summary of CDEI mutational analysis. Compilation of all CDEI single point mutations plus two mutations at positions 9 and 10. Data are taken from the present study (Table 3) and from Hegemann et al. (25). The conserved CDEI sequence is boxed, with the dyad structure indicated by arrows and a diamond. The length of the black bars represents the chromosome fragment mitotic loss rate of each mutation, which is indicated below each bar. The asterisk marks mutations which were analyzed earlier (25) and whose loss rates were recalculated as described in Materials and Methods.

The diploid yeast strain YPH49 is homozygous for the *ade2-101* ocher mutation, leading to red colonies. The presence of one copy of *SUP11* in chromosome fragment-carrying transformants causes pink colonies (Fig. 3D, I and II). Thus, this colony color assay allows determination of the presence of the chromosome fragment, as loss of the chromosome fragment results in a red sector in a pink colony. The comparison of colony-sectoring phenotypes therefore provides a rapid means of estimating the centromere activity of CDEI mutations located on chromosome fragments. This system was used to obtain the first hints on the mitotic loss rate of new *CEN* mutants. The availability of yeast strains carrying various centromere mutations exhibiting mitotic chromosome loss rates between 4.8×10^{-4} and 1.1×10^{-1} (25) (recalculated as described in Materials and Methods) made it possible to draw up a reference list (Table 2). The difference in mitotic loss rates among the mutants was about twofold. New *CEN* mutants created in this study were arranged in a proper order, and subsequently the corresponding mitotic loss per cell division was deduced from the reference list (Table 2). Each mutation is defined by a loss rate range, e.g., CDEI(4-T) has a loss rate of between 1.3×10^{-3} and 2.1×10^{-3}. Small differences in mitotic segregation behavior between certain mutants could therefore not be resolved: CDEI(6-A), CDEI(6-C), and CDEI(5-T) are all in the same mitotic loss rate range of 8.1×10^{-4} to 1.3×10^{-3}.

For rigorous quantification of chromosome segregation ability, we therefore measured all mutants by fluctuation analysis with a modified version of the chromosome fragment assay (25). The dominant cycloheximide sensitivity gene *CYH*^{S}*2* was placed onto pYCF5, yielding pKE5 (Fig. 3B). Upon transformation and chromosome fragmentation, the cycloheximide-resistant yeast strain YJH6 becomes cycloheximide sensitive and cannot grow on plates containing the drug. Loss of the chromosome fragment goes along with growth on cycloheximide plates (Fig. 3D, II). When loss rates were determined several times, they diverged by no more than a factor of 1.1 (data not shown). The cycloheximide R/S system (51) was compared with the original chromosome fragment assay (25) and found to give almost identical results (data not shown), which allows direct comparison of data obtained by either of these systems.

Base pairs forming the CDEI palindrome contribute most to mitotic *CEN* function. Saturation mutagenesis of CDEI immediately revealed that the 6-bp-long inverted repeat (positions 3 to 8) provides the main contribution to centromere activity. It had been shown earlier that single point mutations at positions 7 and 8 reduce centromere activity up to 10-fold (Fig. 4) (25). Single point mutations at positions 3 to 6 (Fig. 2A and Table 3) can reduce chromosome segregation efficiency up to 29-fold [CDEI(3-T)] compared with the wt *CEN6* sequence, with a mitotic chromosome loss rate of 4.8×10^{-4} per cell division. In contrast, changing the conserved base pairs at position 1 or 2 and the nonconserved base pairs at positions 9 and 10 reduces *CEN* function at most twofold [e.g., CDEI(1-T)]. Mutants carrying three of the six mutations at positions 1 and 2 had an activity approximately equal to that of the wt, and one mutant [CDEI(1-C)], at 4.4×10^{-4}, was slightly more active than wt *CEN6*. In five other wt *CEN* DNAs, a G:C instead of an A:T occurs at position 1 (Fig. 1). In accordance with this, the *CEN6* CDEI mutation CDEI (1-G) had a loss rate of 5.1×10^{-4}, which is very close to that of the wt.

Each change of a conserved base pair within the palindrome leads to a reduction in *CEN* function. The extent to which centromere activity is affected is dependent on the particular position in CDEI and the type of mutation introduced. Thus, all three possible single point mutations at position 4 lead to only a 2- to 8-fold reduction in *CEN*

TABLE 3. Chromosome fragment loss rate of CDEI mutations as determined by fluctuation analysis with the cycloheximide R/S system[a]

Yeast strain	Mutation	Mitotic chromosome fragment loss rate
YRN35	wt *CEN6*	4.8×10^{-4}
YRN19	CDEI(1-C)	4.4×10^{-4}
YRN4	CDEI(1-G)	5.1×10^{-4}
YRN3	CDEI(1-T)	8.9×10^{-4}
YRN6	CDEI(2-A)	5.7×10^{-4}
YRN7	CDEI(2-C)	4.8×10^{-4}
YRN8	CDEI(2-G)	6.3×10^{-4}
YRN1	CDEI(3-A)	3.2×10^{-3}
YRN9	CDEI(3-G)	1.2×10^{-2}
YRN2	CDEI(3-T)	1.4×10^{-2}
YRN5	CDEI(4-C)	2.2×10^{-3}
YRS1	CDEI(4-G)	3.7×10^{-3}
YRS2	CDEI(4-T)	1.0×10^{-3}
YRS3	CDEI(5-A)	5.4×10^{-3}
YRS4	CDEI(5-G)	1.8×10^{-3}
YRS5	CDEI(5-T)	1.6×10^{-3}
YRS6	CDEI(6-A)	5.8×10^{-4}
YRS7	CDEI(6-C)	8.6×10^{-4}
YRS8	CDEI(6-T)	6.6×10^{-3}
YRN13	CDEI(9-A)	7.5×10^{-4}
YRN14	CDEI(10-C)	1.0×10^{-3}
YRN12	CDEI(1-G/9-A/10-C)	5.9×10^{-4}

[a] Data were obtained as described in Materials and Methods.

activity, whereas the mutations at position 3 decrease mitotic segregation efficiency between 7- and 30-fold. Of all the palindrome mutations, CDEI(6-A) exhibited the best segregation activity, with a loss rate of 5.8×10^{-4}, which is close to that of wt *CEN6*. This is in agreement with the *CEN* consensus sequence, which allows a purine at this position. At six out of eight positions, a transversion reduces *CEN* activity most strongly, and at four of eight positions, both transversions decrease centromere function more than the remaining transition.

Inspection of the palindromic mutations revealed an imbalance in the contribution of both half-sites to mitotic *CEN* function (Table 3). Mutations in the left half-site, consisting of the sequence CAC at positions 3 to 5, affect centromere activity more than the corresponding symmetric changes in the right half-site, consisting of the sequence GTG at positions 6 to 8. For example, the mutation CDEI(5-G) had a loss rate of 1.8×10^{-3}, while the symmetric mutation CDEI(6-C) exhibited a loss rate of 8.6×10^{-4}. Taking into consideration the mutations at positions 7 and 8, which have been studied previously (25), seven of nine left half-site mutations are more deleterious to *CEN* function than the symmetric right half-site changes. The most drastic difference was found for CDEI(8-A) (loss rate, 2.1×10^{-3}), the symmetrical mutation of which, CDEI(3-T), affects *CEN* function more strongly, by about 6.7-fold (loss rate, 1.4×10^{-2}). The two exceptions to this general finding are both transversions, located at positions 4 and 7 as well as at 5 and 6. Although the palindromic half-sites of CDEI do not contribute equally to mitotic *CEN* function, the pattern of loss rates from the left half-site mutants is reflected in the right half-site loss rate pattern: the mutations having the strongest influence are found at the C:G base pairs (positions 3 and 5) and the symmetric G:C base pairs (positions 6 and 8).

Indications that the functional CDEI sequence is larger than the conserved 8 bp. The saturation mutagenesis of *CEN6* CDEI proved the relevance of the 6-bp palindrome CACGTG at positions 3 to 8 for faithful mitotic chromosome segregation. Since the palindrome is located noncentrally at positions 3 to 8 in CDEI, pointing towards CDEII, we asked ourselves whether an extension of the palindrome to 10 bp, including the highly conserved positions 1 and 2 as well as the nonconserved positions 9 and 10, would be favorable to mitotic *CEN* function. Changing the nonconserved C:G at position 9 to an A:T, which is found in seven other wt *CEN* DNAs, created such a perfect 10-bp palindrome (Fig. 2A). However, analysis of the centromere activity revealed a chromosome fragment loss rate of 7.5×10^{-4}, which is about 1.6-fold higher than the wt rate (Table 3). A second 10-bp palindrome was created (Fig. 2B), which is based on the G:C at position 1 (see consensus sequence, Fig. 1). The triple mutant CDEI(1-G,9-A,10-C) had a loss rate of only 5.9×10^{-4}, better than those of both of the mutants with corresponding single mutations at positions 9 and 10 (Table 3). Interestingly, the single mutation CDEI(10-C) at the nonconserved position 10 had a mitotic loss rate of 1×10^{-3}, which is about 2.1-fold higher than the wt rate and higher than the loss rates of mutants with several changes at 100% conserved positions in CDEI (e.g., positions 2, 4, 6, and 7). Thus, these results indicate that a completely functional *CEN6* CDEI sequence needs, in addition to the eight conserved base pairs, two appropriate base pairs at positions 9 and 10.

Indications for interaction between CDEI and CDEIII DNA-protein complexes. In an attempt to get the first references to the interactions of the CDEI DNA-CPF1 protein complex with the CDEIII-protein complex (24, 41), we introduced mutations in both protein-binding sites (Fig. 2C). If both DNA-protein complexes contribute independently to centromere function, then one would assume in a first approximation that mutations in both binding sites would be additive rather than synergistic. For CDEIII, we chose the mutation CDEIII(15-T), which had been shown previously to strongly affect mitotic chromosome segregation, with a loss rate of 1.1×10^{-1} (25). We combined this primary mutation with eight different CDEI point mutations, all in the left half-site (positions 3 to 5) of the CPF1-binding site, giving mitotic loss rates of between 10^{-3} and 10^{-2}. The colony-sectoring phenotypes of the double mutants immediately revealed their strong impairment in mitotic *CEN* function, and it was impossible to quantify their chromosome loss rates with the cycloheximide R/S system due to extremely high chromosome fragment instability. For all double mutants, the eight single CDEI mutants, and CDEIII(15-T), we therefore determined the percentage of cells without chromosome fragments after selective growth (Fig. 5). This measure of chromosome stability is not as rigorous as the determination of chromosome fragment loss rates by a fluctuation analysis but is useful in determining chromosome stability to a first approximation. For the single CDEI mutations and CDEIII(15-T), we found that between 1 and 11% and 16% of the cells, respectively, had no chromosome fragment, while for wt *CEN6* this number was determined to about 0.2%. In contrast, all double mutants exhibited a much more pronounced chromosome fragment loss, resulting in 60 to 87% of cells without a chromosome fragment. Thus, in the double mutants, the mitotic loss rates of the corresponding single mutations are not additive. This suggests that there are interactions between CDEI and CDEIII DNA-protein complexes.

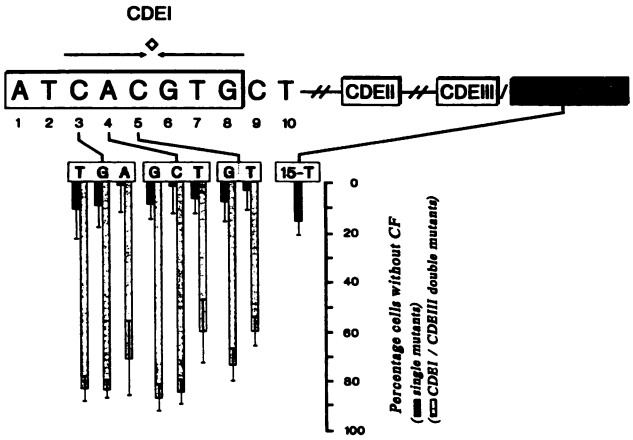

FIG. 5. Comparison of mitotic centromere activities for CDEI single and CDEI-CDEIII double mutations. The percentage of cells without a chromosome fragment (CF) under selective growth conditions represents the degree of centromere activity. Black bars indicate the percentage of cells without a chromosome fragment for the eight single CDEI mutants as well as for the single CDEIII mutant, CDEIII(15-T). Shaded bars represent the corresponding values for the various CDEI-CDEIII(15-T) double mutants. For each mutant, 10 independent selective liquid cultures were analyzed and the mean was calculated. Error bars indicate standard deviation of the mean.

DISCUSSION

The characteristic feature of the 8-bp-long centromere DNA element I is the palindromic sequence CACRTG at positions 3 to 8 (Fig. 2), which suggests recognition and binding by dimers of CPF1, as was found for many procaryotic and eucaryotic transcriptional activator and repressor proteins and their binding sites (28, 44). In fact, retention assays indicate that the HLH protein CPF1 binds to the CDEI-binding site as a homodimer (36).

In CDEI, the palindrome is the main contributor to mitotic *CEN* function. The saturation mutagenesis of the centromere DNA element I presented here verifies the importance of each dyadic base pair for in vivo function, supporting the notion that CPF1 binds as a dimer to this site (36). The compilation of mitotic loss rates obtained for all single point mutations within CDEI shown in Fig. 4 describes the CDEI sequence requirements in *CEN6* for mitotic centromere function. Included are six CDEI mutations which were analyzed earlier (25). The change of each palindromic base pair to any other possible base pair results in an increase in mitotic chromosome fragment loss per cell division. The strongest mutation [CDEI(3-T)] leads to a 29-fold increase in mitotic loss rate compared with the wt rate, and thus it completely inactivates the function of CDEI, as deletion of the whole element results in about the same increase in chromosome loss in the case of *CEN3* (17, 22). A closer inspection of the palindromic mutations reveals that base pair changes in the left half-site generally affect centromere activity more than corresponding symmetrical changes in the right half-site. These differences can vary by as much as about sevenfold [e.g., CDEI(3-T) versus CDEI(8-A)]. The asymmetrical behavior of the half-sites suggests that the in vivo protein-DNA interactions at the half-sites might not be identical. Nevertheless, the pattern of the loss rates obtained for mutations in the left half-site was also found for the right half-site, yet the right half-site mutations affect *CEN* activity less. It remains unclear whether this asymmetry is a property of the CDEI-CPF1 homodimer complex as such or whether it is dependent on the interaction with other centromeric DNA-protein complexes. Recently, a similar situation was found for the CDEIII core sequence, in which a stronger involvement of the right palindromic half-site in mitotic *CEN* function was found (30b). Thus, in CDEI and in CDEIII, the half-sites pointing away from the rest of the *CEN* sequence are more important for mitotic centromere activity than the half-sites facing CDEII. The meaning of these findings is unclear at present.

In CDEI, the strongest mutations for each half-site are found for the two C:G base pairs at positions 3 and 5 as well as for the G:C base pairs at positions 6 and 8. The relevance of these base pairs for CPF1 binding is substantiated by in vivo footprint data, which show these four G nucleotides to be protected against methylation (36, 50), indicative of tight DNA-CPF1 protein interactions. Likewise, in vitro methylation interference experiments with *CEN6* CDEI revealed that methylation of any of the four G nucleotides interferes with CPF1 binding (31). Nevertheless, the G nucleotide at position 6 can be replaced by an A nucleotide, resulting in only a slight increase in loss rate [CDEI(6-A)]. This is in accordance with the consensus sequence, which allows an A or a G at this position.

Conformational flexibility of DNA has been described as a property utilized in specific interactions with proteins. In this type of interaction, the DNA becomes deformed, and mutational analysis of such a DNA-binding site reveals a characteristic substitution pattern, as described for the phage 434 operator/repressor system (1, 32). Since we did not find this pattern for the palindromic base pairs in CDEI, we assume direct interactions of nucleotides with amino acids by either direct readout or indirect readout (43).

The conserved nonpalindromic base pairs at positions 1 and 2 seem to play a subordinate role for mitotic *CEN* function, since their change resulted in an increase in mitotic loss rate of no more than twofold and certain changes had no measurable effect on mitotic *CEN* function. This may indicate an involvement of these base pairs in establishing an optimal DNA conformation needed for binding of the CPF1 protein. Additionally, the high conservation of positions 1 and 2 throughout all *CEN* DNAs may indicate a more important role of these base pairs in meiosis, especially in meiosis I. Indications for an involvement of CDEI in meiosis have been reported (22, 45). Finally, it cannot be excluded that proteins different from CPF1, exhibiting only similar sequence requirements, bind as heterodimers or homodimers to CDEI during meiosis.

Recently, the *CEN* DNA from chromosome 2 was analyzed, and the CDEI sequence was determined to be AT CATGTG, which is identical to the sequence of the *CEN6* mutation CDEI(5-T) (Fig. 2A). Determination of the mitotic loss rate revealed a rate of 4.7×10^{-4} for *CEN2*, which is indistinguishable from that of wt *CEN6* (4.8×10^{-4}) (30a). Interestingly, the *CEN6* mutant CDEI(5-T) exhibits an increased loss rate of 1.6×10^{-3}, or about 3.4-fold higher, clearly indicating that, besides the conserved octanucleotide, additional base pairs are involved in a fully functional CDEI sequence. The mutation CDEI(5-T) has also been introduced into *CEN3*, yielding the sequence GTCATATG, which exhibits wt-like mitotic *CEN* function when analyzed on a chromosome (22) but a significant reduction in the *CEN* plasmid segregation efficiency when analyzed with the plasmid mitotic stability assay. Moreover, in in vitro binding tests, this mutation reduces binding of purified CPF1 protein about 35-fold compared with wt *CEN3* CDEI (2). Thus, the *CEN2*, *CEN3*, and *CEN6* data seem to indicate that the natural CDEI sequences represent CPF1-binding sites, which contain either a perfect 6-bp palindrome (*CEN5*, *CEN6*, *CEN7*, *CEN10*, *CEN14*, and *CEN15*) or an imperfect one with single alterations at position 5 or 6 (*CEN1*, *CEN2*, *CEN3*, *CEN4*, *CEN11*, *CEN13*, and *CEN16*) surrounded by additional base pairs, which are specific and important for each of these *CEN* DNAs.

Our mutational analyses of positions 9 and 10 in *CEN6* CDEI support this idea. The mutations CDEI(9-A) and CDEI(10-C) reduce the chromosome fragment segregation efficiency 1.6-fold and 2.1-fold, respectively, although these positions are not conserved among the *CEN* DNAs. This demonstrates the importance of the neighboring base pairs for complete *CEN* function. Again, in in vivo and in vitro footprint experiments, the wild-type G nucleotide at position 9 in the lower strand is protected against methylation, proving the proximity between this base and the protein (30c, 36). Interestingly, a combination of the two single mutations at positions 9 and 10 with the silent change CDEI(1-G), yielding the triple mutant CDEI(1-G,9-A,10-C), increases the mitotic loss rate only 1.2-fold, resulting in a significantly better *CEN* function than CDEI(9-A) or CDEI(10-C) alone. These results are a first hint of compensatory effects within this DNA-binding site. Such second-site suppression has recently been identified in the centromere DNA element III also (30b).

For CDEII, early data suggested a role as a hinge region,

allowing the interaction of the two DNA-protein complexes at CDEI and CDEIII (21, 45). Additionally, detailed chromatin studies of six different centromeres invariably revealed a region of about 160 bp protected against unspecific (micrococcal nuclease, DNase I) and specific (restriction enzymes) nucleases, covering the three conserved elements CDEI, CDEII, and CDEIII (20, 20a). This may suggest that the protein complexes at CDEI, CDEII (?), and CDEIII interact with each other and perform their activities through a common structure. In vivo analysis of our double CDEI and CDEIII mutants points to such interactions between both DNA-protein complexes (Fig. 5). All double mutations reduce centromere function very strongly compared with the single mutation CDEIII(15-T), which gave a loss rate of 1.1×10^{-1} (Table 2), so the double mutants exhibit almost no *CEN* activity and the effects of the single mutations are not simply additive but rather synergistic. Moreover, the data from Fig. 5 seem to indicate that the influence of the single mutations in CDEI on *CEN* function alters in the double mutants. This again points to the possibility of interactions between the CDEI and CDEIII complexes, but final proof will depend upon identification and characterization of all components of the centromere complex, which may allow the in vitro assembly of this macromolecular structure.

CDEI-like sequences are a widespread protein-binding motif. As in *CEN* DNAs, the sequence RTCACRTG is also found in various yeast promoters. Its role in transcriptional regulation is still unclear, although there are indications of involvement in transcriptional repression in the case of the *GAL2* promoter (36). These CDEI-like sequences exhibit a certain variation at positions 1 and 2, which allows speculation that at these sites, CPF1 may bind together with another protein as heterodimer, or that completely different proteins bind. Recently, a yeast homolog of the human upstream element factor (UEFh), UEFy, was purified and shown to bind to a sequence carrying CACRTG in its central part and to activate transcription (37). Either UEFy is identical to CPF1 or it represents some member of the yeast CDEI-like sequence-binding proteins (11, 18, 42, 49). CDEI-like sequences are also found in higher eucaryotic promoters as a central part of protein-binding sites for different nuclear HLH proteins, many of which have been implicated in the developmental control of gene expression (e.g., E12/E47 [38], MyoD [34], MLTF [12], TDEF [23], TFEB [10], TFE3 [4], and myf5 [7]). In vivo analysis of two different single point mutations in the palindromic binding site CACGTG for the *Xenopus* oocyte-specific TFIIIA distal element factor (TDEF) revealed that changing the central C to an A or the central G to a T reduced the transcription rate in oocytes (23); the same result was obtained for a double point mutation in this binding site (47). All these mutants, when used as competitors in gel shift analyses, competed significantly less well than the wt sequence (23, 47). Comparison of the few data available for the TDEF-binding site with the results obtained by the detailed analysis of CDEI indicates conservation of this DNA-protein recognition system between *S. cerevisiae* and higher eucaryotes.

All CDEI-like sequences found so far fit with the consensus sequence CANNTG. There have been speculations that this core sequence is an essential structural feature common to all of the recognition sequences of various HLH DNA-binding proteins (9). Regarding the CPF1 protein and the centromeric CDEI sequence, our mutational analysis unambiguously proved the relevance of the 6-bp palindrome CACRTG, framed by two additional base pairs on either side, for mitotic centromere function. Based on the results presented here, it is tempting to speculate that the general binding site for HLH proteins consists of the sequence NNCANNTGNN, in which the dinucleotides CA and TG would be involved in the basic recognition, while the remaining DNA sequence would mediate specificity for specific proteins binding as homodimers or as heterodimers.

ACKNOWLEDGMENTS

We are very grateful to P. Philippsen for his support during this work and for many helpful discussions. We thank D. Jäger for communicating the *CEN2* data prior to publication, P. Wenink and P. Philippsen for access to their unpublished data, B. Schweitzer and B. Boschek for critically reading the manuscript, B. Jehn for stimulating conversations, all members of the group for helpful discussions, A. Wilmen for providing us with the yeast strain YJH6, and J. R. Warner for the *CYH*^{s}*2* clone. We thank K. Escher for the synthesis of oligonucleotides, preparation of plasmid pKE5, and general technical assistance; E. Gailhofer and C. Reitz for photographic work; and J. Lauer and D. Wegner for preparation of media.

This work was supported by grants from the Deutsche Forschungsgemeinschaft to J.H.H. (He 1383/2-1 and Sonderforschungsbereich 272).

REFERENCES

1. **Aggarwal, A. K., D. W. Rodgers, M. Drottar, M. Ptashne, and S. C. Harrison.** 1988. Recognition of a DNA operator by the repressor of phage 434: a view at high resolution. Science **242**:899–907.
2. **Baker, R. E., M. Fitzgerald-Hayes, and T. C. O'Brien.** 1989. Purification of the yeast centromere binding protein CP1 and a mutational analysis of its binding site. J. Biol. Chem. **264**:10843–10850.
3. **Baker, R. E., and D. C. Masison.** 1990. Isolation of the gene encoding the *Saccharomyces cerevisiae* centromere-binding protein CP1. Mol. Cell. Biol. **10**:2458–2467.
4. **Beckmann, H., L.-K. Su, and T. Kadesh.** 1990. TFE3: a helix-loop-helix protein that activates transcription through the immunoglobulin enhances μE3 motif. Genes Dev. **4**:167–179.
5. **Bloom, K. S., and J. Carbon.** 1982. Yeast centromere DNA is in a highly ordered structure in chromosomes and small circular minichromosomes. Cell **29**:305–317.
6. **Bram, R. J., and R. D. Kornberg.** 1987. Isolation of a *Saccharomyces cerevisiae* centromere DNA-binding protein, its human homolog, and its possible role as a transcription factor. Mol. Cell. Biol. **7**:403–409.
7. **Braun, T., B. Winter, E. Bober, and H. H. Arnold.** 1990. Transcriptional activation domain of the muscle-specific gene-regulatory protein myf5. Nature (London) **346**:663–665.
8. **Cai, M., and R. W. Davis.** 1989. Purification of a yeast centromere-binding protein that is able to distinguish single base-pair mutations in its recognition site. Mol. Cell. Biol. **9**:2544–2550.
9. **Cai, M., and R. W. Davis.** 1990. Yeast centromere binding protein CBF1, of the helix-loop-helix protein family, is required for chromosome stability and methionine prototrophy. Cell **61**:437–446.
10. **Carr, C. S., and P. A. Sharp.** 1990. A helix-loop-helix protein related to the immunoglobulin E box-binding proteins. Mol. Cell. Biol. **10**:4384–4388.
11. **Chodosh, L. A., S. Buratowski, and P. A. Sharp.** 1989. A yeast protein possesses the DNA-binding properties of the adenovirus major late transcription factor. Mol. Cell. Biol. **9**:820–822.
12. **Chodosh, L. A., R. W. Carthew, J. G. Morgan, G. R. Carbtree, and P. A. Sharp.** 1987. The adenovirus major late transcription factor activates the rat gamma-fibrinogen promoter. Science **238**:684–688.
13. **Clarke, L.** 1990. Centromeres of budding and fission yeast. Trends Genet. **6**:150–154.
14. **Clarke, L., H. Amstutz, B. Fishel, and J. Carbon.** 1986. Analysis of centromeric DNA in the fission yeast *Schizosaccharomyces pombe*. Proc. Natl. Acad. Sci. USA **83**:8253–8257.

15. **Clarke, L., and J. Carbon.** 1980. Isolation of yeast centromere and construction of functional small circular chromosomes. Nature (London) **287**:504–509.
16. **Cottarel, G., J. H. Shero, P. Hieter, and J. H. Hegemann.** 1989. A 125-base-pair *CEN6* DNA fragment is sufficient for complete meiotic and mitotic centromere functions in *Saccharomyces cerevisiae*. Mol. Cell. Biol. **9**:3342–3349.
17. **Cumberledge, S., and J. Carbon.** 1987. Mutational analysis of meiotic and mitotic centromere function in *Saccharomyces cerevisiae*. Genetics **117**:203–212.
18. **Dorsman, J. C., W. C. van Heeswijk, and L. A. Grivell.** 1988. Identification of two factors which bind to the upstream sequences of a number of nuclear genes coding for mitochondrial proteins and to genetic elements important for cell division in yeast. Nucleic Acids Res. **16**:7287–7301.
19. **Fitzgerald-Hayes, M., L. Clarke, and J. Carbon.** 1982. Nucleotide sequence comparisons and functional analysis of yeast centromere DNAs. Cell **29**:235–244.
20. **Funk, M., J. H. Hegemann, and P. Philippsen.** 1989. Chromatin digestion with restriction endonucleases reveals 150–160 bp of protected DNA in the centromere of chromosome 14 in *Saccharomyces cerevisiae*. Mol. Gen. Genet. **219**:153–160.
20a. **Funk, M., J. H. Hegemann, and P. Philippsen.** Unpublished data.
21. **Gaudet, A., and M. Fitzgerald-Hayes.** 1987. Alterations in the adenine-plus-thymine-rich region of *CEN3* affect centromere function in *Saccharomyces cerevisiae*. Mol. Cell. Biol. **7**:68–75.
22. **Gaudet, A., and M. Fitzgerald-Hayes.** 1989. Mutations in *CEN3* cause aberrant chromosome segregation during meiosis in *Saccharomyces cerevisiae*. Genetics **121**:477–489.
23. **Hall, R. K., and W. L. Taylor.** 1989. Transcription factor IIIA gene expression in *Xenopus* oocytes utilizes a transcription factor similar to the major late transcription factor. Mol. Cell. Biol. **9**:5003–5011.
24. **Hegemann, J. H., R. D. Pridmore, R. Schneider, and P. Philippsen.** 1986. Mutations in the right boundary of *Saccharomyces cerevisiae* centromere 6 lead to nonfunctional or partially functional centromeres. Mol. Gen. Genet. **205**:305–311.
25. **Hegemann, J. H., J. H. Shero, G. Cottarel, P. Philippsen, and P. Hieter.** 1988. Mutational analysis of centromere DNA from chromosome 6 of *Saccharomyces cerevisiae*. Mol. Cell. Biol. **8**:2523–2535.
26. **Hieter, P., C. Mann, M. Snyder, and R. W. Davis.** 1985. Mitotic stability of yeast chromosomes: a colony color assay that measures nondisjunction and chromosome loss. Cell **40**:381–392.
27. **Hieter, P., D. Pridmore, J. H. Hegemann, M. Thomas, R. W. Davis, and P. Philippsen.** 1985. Functional selection and analysis of yeast centromeric DNA. Cell **42**:913–921.
28. **Hope, I. A., and K. Struhl.** 1987. GCN4, a eucaryotic transcriptional activator protein, binds as a dimer to target DNA. EMBO J. **6**:2781–2784.
29. **Huberman, J. A., R. D. Pridmore, D. Jäger, B. Zonneveld, and P. Philippsen.** 1986. Centromeric DNA from *Saccharomyces uvarum* is functional in *Saccharomyces cerevisiae*. Chromosoma **94**:162–168.
30. **Ito, H., Y. Fukuda, K. Murata, and A. Kimura.** 1983. Transformation of intact cells treated with alkali cations. J. Bacteriol. **153**:163–168.
30a. **Jäger, D.** 1990. Ph.D. thesis, University of Giessen, Giessen, Federal Republic of Germany.
30b. **Jehn, B., R. Niedenthal, and J. H. Hegemann.** Unpublished data.
30c. **Jiang, W.** 1990. Ph.D. thesis, University of Giessen, Giessen, Federal Republic of Germany.
31. **Jiang, W., and P. Philippsen.** 1989. Purification of a protein binding to the CDEI subregion of *Saccharomyces cerevisiae* centromere DNA. Mol. Cell. Biol. **9**:5585–5593.
32. **Koudelka, G. B., S. C. Harrison, and M. Ptashne.** 1987. Effect of non-contacted bases on the affinity of 434 operator for 434 repressor and Cro. Nature (London) **326**:886–888.
33. **Kramer, W., V. Drutsa, H.-W. Jansen, B. Kramer, M. Pflugfelder, and H.-J. Fritz.** 1984. The gapped duplex DNA approach to oligonucleotide-directed mutation construction. Nucleic Acids Res. **14**:9441–9456.
34. **Lassar, A. B., J. N. Buskin, D. Lockshon, R. L. Davis, S. Apone, S. D. Hauschka, and H. Weintraub.** 1989. MyoD is a sequence-specific DNA binding protein requiring a region of *myc* homology to bind to the muscle creatine kinase enhancer. Cell **58**:823–831.
35. **Lea, D. E., and C. A. Coulson.** 1949. The distribution of the numbers of mutants in bacterial populations. J. Genet. **49**:264–285.
36. **Mellor, J., W. Jiang, M. Funk, J. Rathjen, C. A. Barnes, T. Hinz, J. H. Hegemann, and P. Philippsen.** 1990. CPF1, a yeast protein which functions in centromeres and promotores. EMBO J. **9**:4017–4026.
37. **Moncollin, V., R. Stalder, J.-M. Verdier, A. Sentenac, and J.-M. Egly.** 1990. A yeast homolog of the human UEF stimulates transcription from the adenovirus 2 major late promoter in yeast and in mammalian cell-free systems. Nucleic Acids Res. **18**: 4817–4823.
38. **Murre, C., P. S. McCaw, H. Vaessin, M. Caudy, L. Y. Jan, Y. N. Jan, C. V. Cabrera, J. N. Buskin, S. D. Hauschka, A. B. Lassar, H. Weintraub, and D. Baltimore.** 1989. Interactions between heterologous helix-loop-helix proteins generate complexes that bind specifically to a common DNA sequence. Cell **58**:537–544.
39. **Nakaseko, Y., Y. Adachi, S. Funahashi, O. Niwa, and M. Yanagida.** 1986. Chromosome walking shows a highly homologous repetitive sequence present in all the centromere regions of fission yeast. EMBO J. **5**:1011–1021.
40. **Newlon, C. S.** 1988. Yeast chromosome replication and segregation. Microbiol. Rev. **52**:568–601.
41. **Ng, R., and J. Carbon.** 1987. Mutational and in vitro protein-binding studies on centromere DNA from *Saccharomyces cerevisiae*. Mol. Cell. Biol. **7**:4522–4534.
42. **Ogawa, N., and Y. Oshima.** 1990. Functional domains of a positive regulatory protein, PHO4, for transcriptional control of the phosphatase regulon in *Saccharomyces cerevisiae*. Mol. Cell. Biol. **10**:2224–2236.
43. **Otwinowski, Z., R. W. Schevitz, R.-G. Zhang, C. L. Lawson, A. Joachimiak, R. Q. Marmorstein, B. F. Luisi, and P. B. Sigler.** 1988. Crystal structure of *trp* repressor/operator complex at atomic resolution. Nature (London) **335**:321–329.
44. **Pabo, C. O., and R. T. Sauer.** 1984. Protein-DNA recognition. Annu. Rev. Biochem. **53**:293–321.
45. **Panzeri, L., L. Landonio, A. Stotz, and P. Philippsen.** 1985. Role of conserved sequence elements in yeast centromere DNA. EMBO J. **4**:1867–1874.
46. **Sawadogo, M., and R. G. Roeder.** 1985. Interaction of a gene-specific transcription factor with the adenovirus major late promoter upstream of the TATA box region. Cell **43**:165–175.
47. **Scotto, K. W., H. Kaulen, and R. G. Roeder.** 1989. Positive and negative regulation of the gene for transcription factor IIIA in *Xenopus laevis* oocytes. Genes Dev. **3**:651–662.
48. **Shero, J., M. Koval, F. Spencer, R. Palmer, P. Hieter, and D. Koshland.** 1991. Analysis of chromosome segregation in *Saccharomyces cerevisiae*. Methods Enzymol. **194**:749–773.
49. **Vogel, K., W. Hörz, and A. Hinnen.** 1989. The two positively acting regulatory proteins PHO2 and PHO4 physically interact with *PHO5* upstream activation regions. Mol. Cell. Biol. **9**:2050–2057.
50. **Wenink, P., and P. Philippsen.** Unpublished data.
51. **Wilmen, A., and J. H. Hegemann.** Unpublished data.